Clinical Radiology 74 (2019) 734.e1–734.e6

Contents lists available at ScienceDirect

Clinical Radiology

journal homepage: www.clinicalradiologyonline.net

Parapharyngeal space paraganglioma: distinguishing vagal paragangliomas from carotid body tumours using standard MRI

X. Wang [a], Y. Chen [b], X. Chen [c,*], J. Xian [a,**]

[a] Department of Radiology, Beijing Tongren Hospital, Capital Medical University, Beijing 100730, China
[b] Department of Radiology, Third Affiliated Hospital of Soochow University, Changzhou, Jiangsu 213003, China
[c] Department of Otolaryngology Head and Neck Surgery, Beijing Tongren Hospital, Capital Medical University, Beijing 100730, China

ARTICLE INFORMATION

Article history:
Received 12 February 2019
Accepted 18 April 2019

AIM: To evaluate whether standard magnetic resonance imaging (MRI) could distinguish vagal paragangliomas (VPs) from carotid body tumours (CBTs) in the parapharyngeal space.

METHODS AND MATERIALS: Thirteen VPs in 13 patients and 29 CBTs in 26 patients were included in this study. MRI features were evaluated independently by two head and neck radiologists with 10 and 16 years of experience (X.Wang and Y.Chen).

RESULTS: Significant differences were found in shape, direction of internal carotid artery (ICA) displacement, splaying of the carotid bifurcation, involvement of the jugular foramen, and maximum vertical diameters between VPs and CBTs (p=0.016, <0.001, <0.001, <0.001 and <0.001, respectively). Splaying of the carotid bifurcation was found in all the 29 CBTs for both observers, whereas only four VPs for observer 1 and two for observer 2 showed this feature. The ICA was displaced posteriorly in all the 29 patients with CBTs for both observers, and only three patients with VPs for observer 1 and two for observer 2. Involvement of the jugular foramen was found in seven patients with VPs for both observers, while none of patients with CBT showed this feature. With the combination of splaying of the carotid bifurcation and involvement of the jugular foramen, the multiple logistic regression model revealed the diagnostic accuracy was 95.2% for observer 1 and 97.6% for observer 2. With the combination of ICA displacement direction and involvement of the jugular foramen, the diagnostic accuracy was 97.6% for both observers.

CONCLUSION: MRI features can effectively differentiate VPs from CBTs in the parapharyngeal space.

Introduction

Paragangliomas are highly vascular tumours that can arise in various locations of the paraganglion system.[1] Paragangliomas in the parapharyngeal space of the cervical region mainly include carotid body tumours (CBTs) and

* Guarantor and correspondent: X. Chen, Department of Otolaryngology Head and Neck Surgery, Beijing Tongren Hospital, Capital Medical University, Beijing 100730, China.
** Guarantor and correspondent: J. Xian, Department of Radiology, Beijing Tongren Hospital, Capital Medical University, Beijing 100730, China.
E-mail addresses: trchxh@163.com (X. Chen), cjr.xianjunfang@vip.163.com (J. Xian).

https://doi.org/10.1016/j.crad.2019.04.018
0009-9260/

vagal paragangliomas (VPs). Vagal paragangliomas, arising from paraganglia along the vagus nerve, are less common than CBTs, representing approximately 5–11% of all head and neck paragangliomas.[2,3]

Although VPs and CBTs are both paragangliomas pathologically, the treatments and prognoses are different in many ways.[1–6] CBTs are the most accessible head and neck paraganglioma, so can be removed more easily at surgery. By contrast, treatment of VPs is challenging due to involvement of multiple cranial nerves and the skull base.[2,3,5] Thus, therapeutic radiation is recommended as a first-line approach.[6] Surgery is performed when tumours enlarge rapidly and when large tumours compress vital structures. Surgery of VPs is usually accomplished through a lateral approach with removal of the associated vagus nerve, creating unilateral vocal fold paralysis and pharyngeal plexus deficit. Thus, morbidity related to resection of VPs is significantly higher compared with CBTs.[7] It has been reported that a postoperative vagal deficit is almost universal by either paresis or necessary sacrifice during surgery.[8,9] Therefore, differentiating VPs from CBTs is of crucial importance for prognosis and treatment choice.

The computed tomography (CT) and magnetic resonance imaging (MRI) features of VPs have been reported in a few of studies.[1,3,7,10,11] High-resolution CT is of limited value in the characterisation of soft-tissue masses due to poor soft-tissue contrast resolution, although CT can be a valuable adjunct to MRI, especially in evaluating bony involvement at the skull base. MRI is now widely accepted as the best method for the characterisation of a soft-tissue mass. It has been reported that CBTs can cause splaying of the carotid bifurcation, contrary to vagal paragangliomas, which cause displacement of the internal carotid artery (ICA) anteriorly with no increase of the distance between the internal and external arteries, which can be appreciated at MRI; however, a previous study also reported that VPs occasionally may masquerade as CBTs by splaying apart the internal and external carotid arteries.[11] Thus, whether these imaging features can completely distinguish CBT from VPs remains to be determined. Therefore, the aim of the present study was to examine whether standard MRI could provide effective differentiation between CBTs and VPs.

Methods and materials

Patients

The hospital's database was reviewed and all patients who met the following criteria during a 10-year period (between September 2008 and July 2018) were identified: (1) a mass was demonstrated in the parapharyngeal space at MRI; (2) surgical histopathological evaluation and intraoperative findings confirmed the diagnosis of a VP or a CBT; (3) no biopsy or therapy was initiated before the MRI. Malignant paragangliomas were excluded. Finally, 39 patients with 42 paragangliomas were enrolled retrospectively in the study, consisting of 13 patients with 13 VPs (one men and 12 women; average age, 44.2±12.1 years) and 26 patients with 29 CBTs (11 men and 18 women; average age 44.6 ±10.8 years). Bilateral CBTs were seen in three patients. This retrospective study was approved by the institutional review board with waiver of informed consent.

The clinical data including clinical presentations, physical examinations, and operative recordings were extracted from the medical records. The resection of all the 29 CBTs was performed via a transcervical approach. Surgical approaches used for VPs included: transcervical approach in eight cases, transcervical–transmastoid approach in four cases, and type A infratemporal fossa approach in one case.

MRI protocol

MRI was performed on a GE HDxt 3 T MRI system (GE Healthcare, Milwaukee, WI, USA) in 24 patients and an Ingenia 3 T MRI system (Philips Healthcare, Amsterdam, Netherlands) in 15 patients with an eight-channel head and neck coil. Unenhanced axial and coronal T1-weighted imaging (WI), axial T2WI and enhanced axial, coronal, and sagittal T1WI were performed in all patients. The parameters on the GE HDxt 3 T MRI system were as follows: fast spin echo (FSE) T1WI: 600–700 ms repetition time (TR), 8 ms echo time (TE); FSE T2WI: 3,900–4,300 ms TR, 90 ms TE; 320×224 matrix, 20×20 cm field of view, 4–5 mm section thickness, 1 mm gap. The parameters on the Ingenia 3 T MRI were as follows: turbo spin echo (TSE) T1WI: 600–650 ms TR, 7 ms TE; TSE T2WI: 2,500–3,000 ms TR, 80 ms TE; 276×216 matrix, 20×20 cm field of view, 5 mm section thickness, 1 mm gap.

Gadopentetate dimeglumine (Magnevist; Bayer Schering, Berlin, Germany) was injected intravenously (0.1 mmol/kg) with an injection flow rate of 2 ml/s.

Imaging analysis

The MRI images were analysed by two authors independently (X.Wang. and Y.Chen.) with 10 and 16 years of experience in head and neck imaging, respectively. MRI features including side, shape, T1 signal intensity, T1 homogeneity, T2 signal intensity, T2 homogeneity, flowing void effect, pattern of enhancement, splaying of the carotid bifurcation, encasement of the internal carotid arteries, displacement direction of the ICA, and involvement of the jugular foramen were analysed. The maximum vertical diameters of VPs and CBTs were measured on the sagittal contrast-enhanced MRI images.

Statistical analysis

Chi-square tests and a Mann–Whitney *U*-test were used to test differences in the MRI features between CBTs and VPs. A univariate analysis was used to determine the statistically significant variables ($p<0.05$) to model the probability of VPs versus CBTs, which were then used to fit a multivariate logistic regression model. Kappa analysis and intraclass correlation coefficient (ICC) were used to evaluate inter-reader reproducibility for MRI features. The kappa and ICC values were interpreted as follows: 0, no agreement;

0.01–0.20, slight agreement; 0.21–0.40, fair agreement; 0.41–0.60, moderate agreement; 0.61–0.80, substantial agreement; and 0.81–1.00, almost perfect agreement. All statistical analyses were performed with SPSS 17.0 (SPSS, Chicago, IL, USA) software.

Results

Clinical data of VPs and CBTs

Clinical presentation for VPs was an asymptomatic neck mass (7/13,53.8%), followed by hoarseness (4/13,30.8%), pharyngeal foreign body sensation (2/13,15.4%), and headache (1/13,7.7%). The most frequent presenting symptom of CBT was an asymptomatic slow-growing neck mass (24/26,92.3%), followed by hoarseness (1/26, 3.85%) and pulsatile tinnitus (1/26, 3.85%). No significant difference was found in age and sex between CBTs and VPs (p=0.892 and 0.067, respectively).

MRI findings of VPs and CBTs

MRI features of VPs and CBTs, and interobserver agreement between observers 1 and 2 were demonstrated in Table 1. Significant differences were found in shape, direction of ICA displacement, splaying of the carotid bifurcation, and involvement of the jugular foramen between VPs and CBTs (p=0.016, <0.001, <0.001, and <0.001, respectively). Anterior displacement of the ICA, involvement of the jugular foramen, and irregular shape correlated with VPs (Fig 1), whereas posterior displacement of the ICA, splaying of the carotid bifurcation and regular shape were predictive of CBTs (Fig 2). Splaying of the carotid bifurcation were found in all the 29 CBTs for both observers, whereas only four VPs for observer 1 and two for observer 2 showed splaying of the carotid bifurcation. The ICA was displaced posteriorly in all the 29 patients with CBTs; and only three VPs for observer 1 and two for observer 2 showed this feature. Involvement of the jugular foramen was found in seven patients (7/13, 53.8%) with VPs for both observers, while none of patients with CBT showed this feature. The maximum vertical diameters of the VPs (6.17±1.45 cm) were significantly larger than those of the CBTs (3.93±1.81 cm; p=0.000). Almost perfect agreement was achieved for maximum vertical diameters (ICC=0.945).

With the combination of splaying of the carotid bifurcation and involvement of the jugular foramen, multiple logistic regression models revealed the diagnostic accuracy was 95.2% (sensitivity, 84.6%; specificity 100%) for observer 1 and 97.6% (sensitivity, 92.3%; specificity 100%) for observer 2, respectively. With the combination of ICA displacement direction and involvement of the jugular foramen, the diagnostic accuracy was 97.6% (sensitivity, 92.3%; specificity 100%) for both observers. No significant difference was found in these logistic regression models (p=1.000 for both observers).

Table 1
MRI findings of VPs and CBTs in the parapharyngeal space.

MRI features	CBT		VP		p-Value	κ
	n	%	*n*	%		
No. of tumours	29	100	13	100		
Side					0.616	1.00
Right	11	38	6	46		
Left	18	62	7	54		
Shape					0.016	0.54
Regular	16	55	2	15		
Irregular	13	45	11	85		
T1 signal intensity					0.456	0.86
Hypointense	13	45	8	62		
Isodense	15	52	5	38		
Hyperintense	1	3	0	0		
T1 homogeneity					0.314	0.62
Homogeneous	17	59	10	77		
Inhomogeneous	12	41	3	23		
T2 signal intensity					0.562	0.65
Hypointense	6	21	2	15		
Isodense	3	10	3	23		
Hyperintense	20	69	8	62		
T2 homogeneity					0.559	0.54
Homogeneous	4	14	1	8		
Inhomogeneous	25	86	12	92		
Flowing void effect					0.719	0.61
Yes	10	34	3	23		
No	19	66	10	77		
Encasement of ICA						0.74
Yes	22	76	6	46		
No	7	24	7	54		
Direction of ICA displacement					<0.001	0.94
Posteriorly	29	100	3	23		
Anteriorly	0	0	10	77		
Splaying of carotid bifurcation					<0.001	0.81
Yes	29	100	4	31		
No	0	0	9	69		
Involvement of jugular foramen					<0.001	1.00
Yes	29	100	7	54		
No	0	0	6	46		
Pattern of enhancement						0.232
Homogeneous	8	28	1	8		
Inhomogeneous	21	72	12	92		

VP, vagal paragangliomas; CBT, carotid body tumour; ICA, internal carotid artery.

Discussion

In the present study cohort, differences were found in direction of ICA displacement, splaying of the carotid bifurcation, involvement of the jugular foramen, shape, and maximum vertical diameter between VPs and CBTs, although no difference was found in signal intensity characteristics. All the CBTs showed posterior displacement of the ICA and splaying of the carotid bifurcation, although most of VPs demonstrated anterior displacement of the ICA without splaying of the carotid bifurcation. Involvement of the jugular foramen correlated with VPs, while no patient with CBT showed this feature. With combination of these MRI features, VPs can be differentiated effectively from CBTs in the parapharyngeal space.

VPs are rare hypervascular tumours arising from paraganglionic tissue associated with one of the three ganglia of the vagus nerve.[11] It has been reported that the most

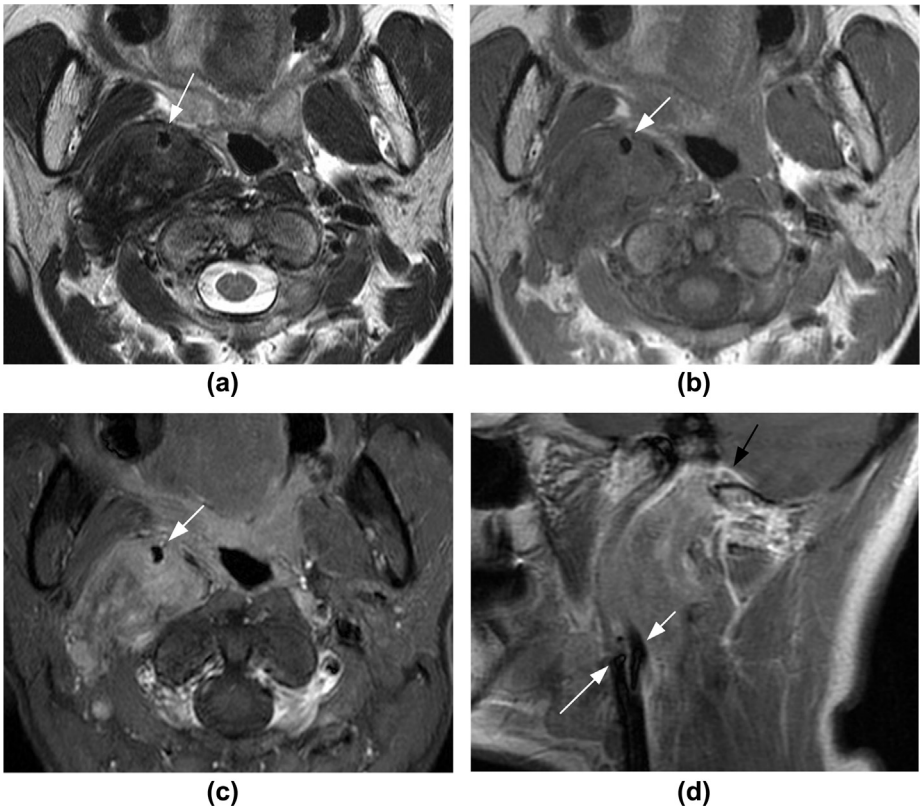

Figure 1 MRI images of a 28-year-old woman with a VP. (a) Axial T2-weighted MRI image demonstrates a heterogeneous hypointense mass relative to grey matter in the right parapharyngeal space. (b) Transverse T1-weighted MRI image shows the mass with inhomogeneous isointensity. (c) Axial contrast-enhanced fat-suppressed T1-weighted MRI image shows a heterogeneously enhanced tumour. (a–c) Arrows indicate anterior displacement of the ICA. (d) Sagittal contrast-enhanced T1-weighted MRI image shows anterior displacement of the ICA (short arrow) and no increase of the distance between the ICA and external carotid artery (long arrow). Involvement of the jugular foramen is visible (black arrow). Histopathological examination revealed a vagal paraganglioma with fibrous connective tissue proliferation and fibrosis interspersed in the tumour stroma.

frequent presenting symptom of VP is a painless neck mass, followed by hoarseness due to vagus nerve affection.[7] Consistent with previous studies, the present results showed the most common clinical presentation of VPs was an asymptomatic neck mass (53.85%) followed by hoarseness (30.77%), with hoarseness more common in VPs compared with CBTs (3.85%).

The treatment of VPs is challenging, because VPs originate from the vagus nerve and often involve multiple cranial nerves. Due to the associated speech and swallowing morbidity following VP resection, surgery is now less commonly recommended. Surgery is only recommended in rapidly enlarging VPs and large VPs compressing vital structures via a transcervical approach. Sometimes, a transcervical–transmandibular or a type A infratemporal fossa approach is used in VPs involving the jugular foramen. In other cases, therapeutic radiation is recommended as a first-line approach.[6] In contrast to the situation with VPs, there is a consensus in that the treatment choice for CBTs is surgical resection using a cervical approach. CBTs are easily removed due to their location away from the skull base. Thus, preoperative determination of origination of parapharyngeal paraganglioma, a CBT or a VP, is critical for treatment choice.

MRI, as the best technique for the characterisation of a soft-tissue mass, has been reported to play an important role in the characterisation of parapharyngeal tumours,[12] the majority of which are pleomorphic adenomas, schwannomas, and paragangliomas. Pleomorphic adenomas, which are located in the prestyloid parapharyngeal space, displace the ICA posteriorly with no splaying of the carotid bifurcation. Schwannomas demonstrate hypointense on T1WI, hyperintense on T2WI, and heterogeneous enhancement with the ICA displaced anteriorly. Generally, paragangliomas can be easily differentiated from pleomorphic adenomas and schwannomas with characteristic imaging findings of low signal intensity on T1WI, high signal intensity on T2WI, intensive contrast enhancement, “salt pepper appearance” representing flow voids, and encasement of the ICA. The MRI features of the two types of paragangliomas, CBTs and VPs, are similar. Their differentiation relies on displacement of vessels. VPs tend to occupy the poststyloid parapharyngeal space and typically displace the carotid system anteromedially. CBTs, as an enhancing soft-tissue tumour at the level of the carotid bifurcation, show splaying of the ICA and external carotid artery with posterior displacement of the ICA; however, previous studies have also showed that VPs may occasionally masquerade as

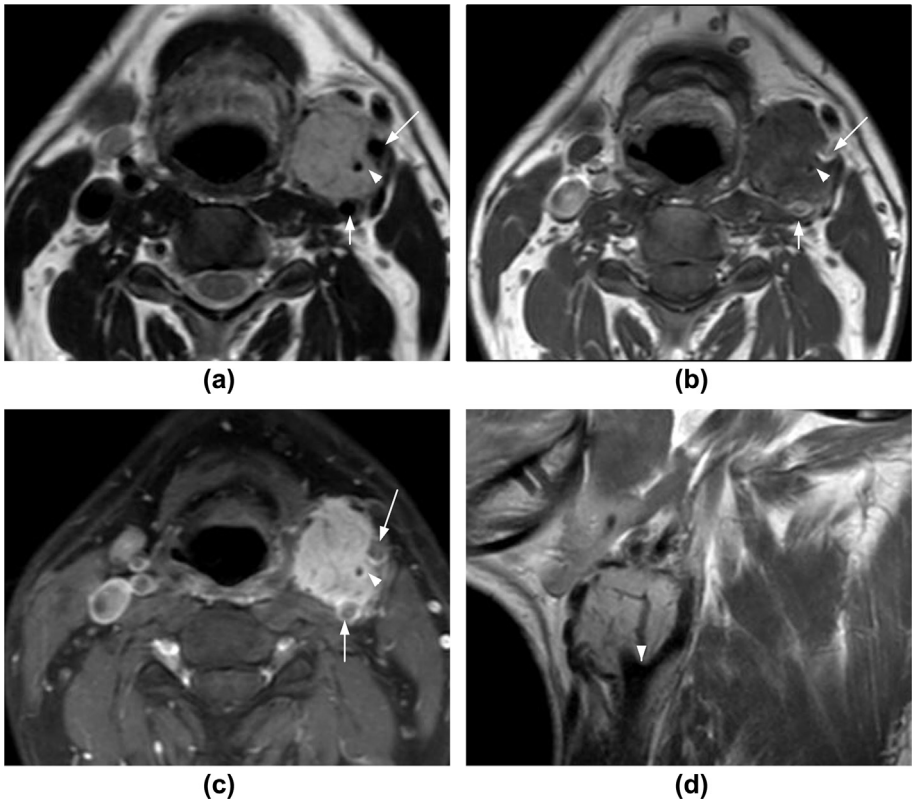

Figure 2 A 62-year-old woman with a CBT in the left parapharyngeal space. (a) Transverse T2-weighted MRI image shows a heterogeneous hyperintense mass relative to grey matter. (b) Transverse T1-weighted MRI image shows the mass with heterogeneous hypointensity. (c) Axial contrast-enhanced fat-suppressed T1-weighted image shows obvious enhancement of the mass. (a–c) Increase of the distance between the ICA (short arrow) and external carotid artery (long arrow) and flowing void effect (arrowhead) are visible. (d) Sagittal contrast-enhanced T1-weighted MR image shows the mass is located at the carotid bifurcation with splaying of the carotid bifurcation (arrowhead).

CBTs by splaying apart the ICA and external carotid artery.[11,13] In the present study, splaying of the carotid bifurcation was found in a small number of patients with VPs (four cases for observer 1 and two for observer 2). Although with splaying of the carotid bifurcation, three of the four VPs showed anterior displacement of the ICA. Thus, not only splaying of the carotid bifurcation but also direction of ICA displacement should be considered in the diagnosis of VPs in clinical decision-making.

Based on the present results, a more irregular shape and larger vertical diameter were predictive of VPs. This is probably because VPs arise from paraganglionic tissue and extend along the vagus nerve resulting in vertical growth faster than horizontal growth. When the tumour grows along the vagus nerve to the level of the skull base, involvement of the jugular foramen is found.

The signal intensity features of VPs were the same as those of CBTs, as they are both paragangliomas histologically: homogeneous low-to-moderate signal intensity on T1WI, inhomogeneous high signal intensity on T2WI, heterogeneous enhancement, flowing void effect, and encasement of the ICA. Flowing void effect due to vascularisation of paragangliomas, known as “salt and pepper” pattern, has been reported in many studies.[7,9–11] Consistent to previous studies, it was found in 10 cases of 29 CBTs (34%) and three cases of 13 VPs (23%) in present study. Six cases of CBTs and two cases of VPs showed low signal intensity on T2WI. This was probably caused by the extensive stromal fibrosis in the tumour, known as sclerosing paraganglioma.[14]

Multicentric tumours occur in 10–20% of all head and neck paragangliomas and bilateral tumours have been reported in 4.4% of sporadic cases.[15] In the present study, bilateral CBTs were seen in three patients (3/39, 7.7%). Management of multiple paragangliomas is more challenging. Different surgical approaches are applied for multiple paragangliomas in different sites including jugulotympanic paragangliomas, CBTs, and VPs. Thus, main goals of imaging are to locate the tumours accurately and to aid the clinical diagnosis in different sites.

The present study had several limitations. First, the MRI examinations were acquired using two different MRI systems. Second, because the sample size of the VPs was relatively small, only two unrelated MRI features can be chosen for each stepwise multiple logistic regression model. Further studies on larger numbers of tumours need to be conducted. Finally, MR angiography was not performed in this study. Although a previous study[16] showed that, for detecting paragangliomas, the sensitivity of MR angiography was better than that of a standard imaging protocol, it was not conducted in present study due to that the aim was to characterise VPs rather than detect multiple paragangliomas.

In conclusion, MRI features can effectively differentiate VPs from CBTs in the parapharyngeal space. VPs should be considered in clinical decision-making if a parapharyngeal paraganglioma shows anterior displacement of the ICA, no splaying of the carotid bifurcation, or jugular foramen involvement.

Conflict of interest

The authors declare no conflict of interest.

Acknowledgements

This work was supported by the High Level Health Technical Personnel of Bureau of Health in Beijing (grant number 2014-2-005); Beijing Municipal Administration of Hospitals Clinical Medicine Development of Special Funding Support (grant number ZYLX201704); National Key Technology Research and Development Program of the Ministry of Science and Technology of China (grant number 2015BAll6H00); "Key Talent Project" of Beijing (grant number 2014001).

References

1. van den Berg R. Imaging and management of head and neck paragangliomas. *Eur Radiol* 2005;**15**(7):1310–8.
2. Hu K, Persky MS. Treatment of head and neck paragangliomas. *Cancer Control* 2016;**23**(3):228–41.
3. González-Orús Álvarez-Morujo R, Arístegui Ruiz M, Martin Oviedo C, *et al*. Management of vagal paragangliomas: review of 17 patients. *Eur Arch Otorhinolaryngol* 2015;**272**(9):2403–14.
4. Williams MD. Paragangliomas of the head and neck: an overview from diagnosis to genetics. *Head Neck Pathol* 2017;**11**(3):278–87.
5. González-Orús Álvarez-Morujo RJ, Arístegui Ruiz MÁ, da Costa Belisario J, *et al*. Head and neck paragangliomas: experience in 126 patients with 162 tumours. *Acta Otorrinolaringol Esp* 2015;**66**(6):332–41.
6. Taïeb D, Kaliski A, Boedeker CC, *et al*. Current approaches and recent developments in the management of head and neck paragangliomas. *Endocr Rev* 2014;**35**(5):795–819.
7. Moore MG, Netterville JL, Mendenhall WM, *et al*. Head and neck paragangliomas: an update on evaluation and management. *Otolaryngol Head Neck Surg* 2016;**154**(4):597–605.
8. Varoquaux A, Kebebew E, Sebag F, *et al*. Endocrine tumours associated with the vagus nerve. *Endocr Relat Cancer* 2016;**23**(9):R371–9.
9. Capatina C, Ntali G, Karavitaki N, *et al*. The management of head-and-neck paragangliomas. *Endocr Relat Cancer* 2013;**20**(5):R291–305.
10. Varoquaux A, Fakhry N, Gabriel S, *et al*. Retrostyloid parapharyngeal space tumours: a clinician and imaging perspective. *Eur J Radiol* 2013;**82**(5):773–82.
11. Sniezek JC, Netterville JL, Sabri AN. Vagal paragangliomas. *Otolaryngol Clin North Am* 2001;**34**(5):925–39.
12. Muraz E, Delemazure AS, Mourrain-Langlois E, *et al*. Peripharyngeal space tumours: can magnetic resonance and multidetector-row computed tomography help predict location, malignancy and tumour type? *Diagn Interv Imaging* 2016;**97**(6):617–25.
13. Kerr JT, Eusterman VD, Yoest SM, *et al*. Pitfalls in imaging: differentiating intravagal and carotid body paragangliomas. *Ear Nose Throat J* 2005;**84**(6):348–50.
14. Ng E, Duncan G, Choong AM, *et al*. Sclerosing paragangliomas of the carotid body: a series of a rare variant and review of the literature. *Ann Vasc Surg* 2015;**29**(7). 1454.e5-1454.e12.
15. Szymańska A, Szymański M, Czekajska-Chehab E, *et al*. Diagnosis and management of multiple paragangliomas of the head and neck. *Eur Arch Otorhinolaryngol* 2015;**272**(8):1991–9.
16. van den Berg R, Verbist BM, Mertens BJ, *et al*. Head and neck paragangliomas: improved tumour detection using contrast-enhanced 3D time-of-flight MR angiography as compared with fat-suppressed MRI techniques. *AJNR Am J Neuroradiol* 2004;**25**(5):863–70.